Time integrated transient reflectivity *versus* ablation characteristics of Borofloat, BK7, and B270 optical glasses ablated by 34 fs pulses

A. ANDRÁSIK,[1,2,*] R. FLENDER,[1] J. BUDAI,[1] T. SZÖRÉNYI,[1] AND B. HOPP[1]

[1]*Department of Optics and Quantum Electronics, University of Szeged, H-6720 Szeged, Dóm tér 9., Hungary*

[2]*Department of Photonics and Laser Research, Interdisciplinary Excellence Centre, University of Szeged, Hungary*

[*]*andrasika@titan.physx.u-szeged.hu*

Abstract: Ablation and plasma mirror characteristics of Borofloat, BK7, and B270 glasses processed with 34 fs pulses of 800 nm central wavelength are compared in the 10^{14}–10^{15} W/cm^2 intensity domain. With thresholds of 1.7-1.9$\times 10^{14}$ W/cm^2, higher than those of fused silica, and depths saturating above 5×10^{14} W/cm^2, the three glasses behave similarly from the point of view of ablation. With reflectivity enhancements comparing favorably with that of fused silica, the glasses prove to be good plasma mirror hosts. With the steepest increase in time integrated transient reflectivity with intensity, Borofloat is the most promising candidate.

1. Introduction

The plasma mirror, PM technique has successfully been applied for the improvement of the temporal contrast [1–6]. A bottleneck is the damage of the hosting surface due to the concomitant ablation. Since each shot reduces the area available, when working at high repetition rate the target will rapidly be consumed. There is therefore a demand for commercially available, cheap target materials, possessing appropriate plasma mirror characteristics together with the possibility of surface regeneration. When assessing the competitiveness of the candidates the behavior of the transient reflectivity and the response of the material to the ablating laser pulse should be considered correspondingly.

Already early studies on the effect of pulse duration [7–12] revealed that the smaller the pulse duration the higher was the intensity required to ignite ionization, i.e. PM formation. The dependence of the transient reflectivity of the plasma on laser intensity/fluence was mainly recorded for fused silica targets [10–19]. There were several attempts to find self-healing alternatives with appropriate PM properties, like water [5,20], organic fluids [2,5], polymers [4], liquid crystal [21] and VHS tape [22]. Optical glasses received astonishingly little attention: we could find data only for BK7 glass [23,24].

The effect of pulse duration on the ablation characteristics of dielectrics has also a long history [25–34] revealing that pulse shortening results in more deterministic [32,35] and cleaner [33,35] ablation. The variance in the response of different target materials to irradiation with ultrashort pulses was examined as well [16,36–38]. Single pulse ablation characteristics of silica have been reported [16,30,33–35,37,39–45]. CaF$_2$ [46], sapphire [16,40,47], various types of glasses [38,41,42,48–51] and even polymers, e.g. PET [52] and PMMA [53] were also investigated in the intensity domain of PM formation.

While showing a wide diversity of process parameters all papers cited above are in accord in describing either the optical response or the ablation characteristics of the materials investigated. There were very few attempts to connect both aspects e.g. [17,18,34]. In this paper we report a

comparative study connecting the PM and single-shot ablation characteristics of three optical glasses considered as promising candidates for replacing fused silica in plasma mirror based contrast enhancement.

2. Experimental

A modelocked laser oscillator (Spectra-Physics Rainbow CEP4, 800 nm), and Ti:sapphire based CPA amplifier operating in the TeWaTi laser lab at University of Szeged [54] provided 34 ± 0.16 fs pulses with 1 mJ maximum pulse energy. The energy stability at the output of the amplifier was better than 1% (RMS). The temporal contrast of the pulses after amplification was 10^7 measured by a third order cross-correlator (SEQUOIA from Amplitude Technologies). The experimental setup is sketched in Fig. 1. In order to select single pulses from the output of the amplifier the repetition rate was decreased to 1 Hz and an optical shutter (Thorlabs Inc. SH05) with a benchtop shutter controller (Thorlabs Inc. SC10) was used. Reliable and reproducible variation of the pulse energy was achieved by a polarization-rotation based beam attenuator. Pulse energies tuned from 90 up to 430 µJ were measured with a Gentec QE50SP-H-MT-V0 energy meter right after the attenuator with relative deviation better than 5%. An off-axis parabolic mirror (Thorlabs Inc. MPD169-P01) focused the beam onto the target placed before the focal plane, i.e. in converging beam path. The reflected focal length (RFL) of the focusing mirror is 152.4 mm which allows focusing of the beam with an F-number of f/19.
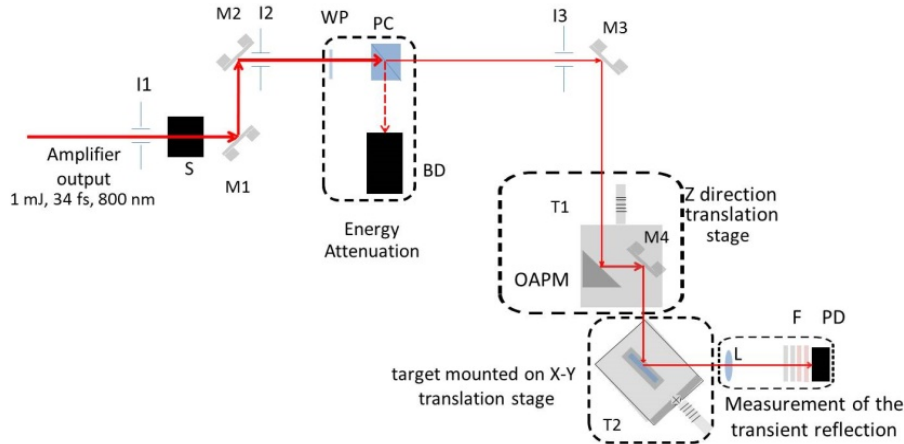

Fig. 1. Scheme of the setup. M1-M4: flat silver mirrors; I1- I3: iris diaphragms; S: optical shutter; WP: half-wave plate; PC: polarization beamsplitter cube; BD: beam dumper; T1: translation stage toward z-direction; T2: translation stages toward x-y directions; OAPM: off-axis parabolic mirror; L: bi-convex lens; F: filters; PD: photodiode.

Uncoated optical glass pieces of Schott's BOROFLOAT (Edmund Optics #48-542) N-BK7 (Eksma Optics #215-0222) and B270 Superwhite (Edmund Optics #48-538) were used as targets at 45° angle of incidence. Pristine surface was ensured shot-to-shot by positioning the target using translation stages. The beam reflected from the sample surface was focused onto the photodiode PD (Thorlabs DET36/A) by a lens of 35 mm focal length and 25.4 mm aperture size. Longpass filters with cutoff wavelength of 620 nm were applied to exclude the light of the plasma while reflective filters in front of the photodiode reduced the intensity to appropriate levels. Therefore the signal detected by PD scales with the energy reflected from the processed target.

At each pulse energy 11 holes were ablated firing 11 individual pulses onto the target surface. The shape of the ablated holes was characterized by a Veeco DEKTAK8 stylus profilometer. The actual traces were recorded with 0.1 nm vertical and 0.17 µm lateral resolution. The diameter

and depth values defined as the distance between the two points where the trace crosses the zero height level and the maximal difference between the zero level and the deepest point of the trace, respectively, were derived from line scans at the center of the spots along the minor axes. Note that the deepest point and the center of a hole did not necessarily coincide. The diameter and depth data given below are 11 holes averages.

To determine the actual diameter of the beam on the sample surface the well-known expression connecting the ablated hole diameter with the fluence, and thus pulse energy was applied [55]:

$$D^2 = 2w^2 ln(F/F_{th}), \tag{1}$$

where w is $1/e^2$ beam radius while F and F_{th} stand for the peak and ablation threshold fluencies, respectively. In Fig. 2 a linear relationship with the logarithm of the energy is clearly visible, indicating that even though the measurements were carried out in air, nonlinear effects were not occurring.

The actual peak fluencies and peak intensities were calculated by the diameter-regression technique [44] according to the following expressions:

$$F = 2E_p/(\pi w^2 \sqrt{2}), \tag{2}$$

$$I = 2E_p/(\pi w^2 \tau \sqrt{2}), \tag{3}$$

where E_p denote the pulse energy and τ is the full width of half maximum (FWHM) pulse duration, taking into account the actual spot radii on the surface (25.1, 26.05 and 24.83 µm) for Borofloat, BK7 and B270, respectively.
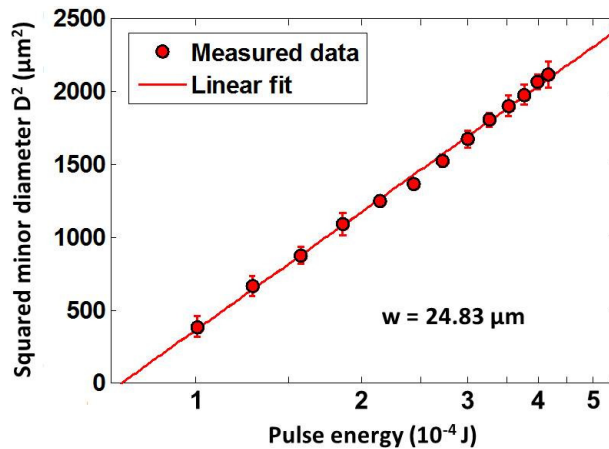

Fig. 2. Determination of the beam radius on the surface of the B270 glass target using linearization of the recorded hole diameters.

3. Results

In Fig. 3 the diameter and the depth of the ablated holes are plotted together with the photodiode signal as a function of laser intensity for the three glasses. In order to demonstrate the repeatability of the experiments, two diameter/depth/PD signal vs. intensity functions are presented for each glass derived from two independent measurement series in which each data point has been calculated as the average of the respective diameter/depth/PD signal value measured on 11 holes ablated with the same intensity. The two series appear in Fig. 3 as triangles and circles. The measurement error was generally less than the symbols.
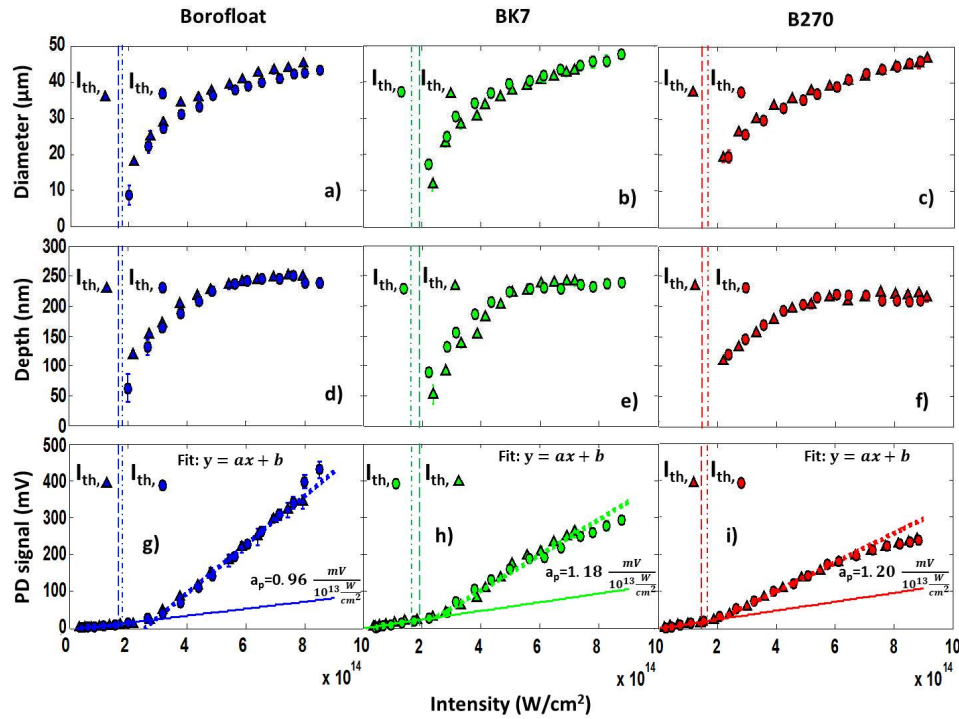
Fig. 3. Ablation and transient reflectivity characteristics of the glasses investigated. Minor diameter: a-c, maximal depth: d-f of the ablated holes and the reflected signal: g-i for BOROFLOAT, BK7 and B270 targets, respectively.

The ablation characteristics proved to be very similar. The threshold intensities have been determined from the intensity dependence of hole diameters using the regression technique [e.g. 44]. The $1.72 \pm 0.06 \ 10^{14}$, $1.89 \pm 0.16 \ 10^{14}$ and $1.75 \pm 0.09 \ 10^{14}$ W/cm^2 values calculated as averages of the thresholds derived for the two series (indicated as vertical dashed and dash-dotted lines in Fig. 3.) for Borofloat, BK7 and B270, respectively, are equal within measurement error. Above the ablation threshold the diameter values follow the well-known logarithmic dependence [37,44,48,55,56] in the whole range investigated reaching similar values around 45 µm at 9×10^{14} W/cm^2. The depths increase with increasing intensity and – contrary to the diameters – show saturation which starts at slightly different intensities: above 6×10^{14}, 5.5×10^{14} and 5×10^{14} W/cm^2 for Borofloat, BK7 and B270, respectively. The maximal depth values decrease moderately in the Borofloat-BK7-B270 order reaching 250, 240 and 220 nm, respectively. The corollary: the Borofloat, BK7 and B270 glasses behave similarly from the point of view of ablation.

The photodiode signal vs. intensity functions can be fitted by two straight sections with different slopes joining in the vicinity of the ablation threshold for all glasses (Figs. 3(g)–3(i)). The fits have been calculated taking into account the data points of both series. Below the threshold the slopes of the curves differ only slightly, while clearly deviating when exceeding it. As seen in Figs. 3(g)–3(i) the ratio of the slopes of the three straight lines representing the extrapolation of the first sections of the fits (solid lines): 0.96:1.18:1.20 well coincides with the ratio of the absolute values of the front side permanent reflectivities of the p-polarized beam at 45° of the respective glasses: 0.0068:0.0089:0.0093 as measured by spectroscopic ellipsometry. The dependence of the PD signal as a function of intensity below the ablation threshold can thereby be associated with the change in the permanent reflectivity.

The emergence of the plasma mirror results in a steep increase in the reflectivity above the threshold. This increase is the most significant for the Borofloat glass, while the smallest slope appears for B270. Accordingly, the PD signal reaches the largest values in the case of the Borofloat samples at 400 mV, while the maxima are 300 and 250 mV for BK7 and B270, respectively. For the latter two the reflectivity saturates at the highest intensities, which along the different slopes and maxima emphasizes the different reflectivity behavior of the three glasses.

4. Discussion

4.1. Ablation characteristics

The model material of the ultrashort pulse ablation of dielectrics is fused silica [16,30,33–35,37,39–45]. A comparison of the results is nevertheless hardly feasible due to the diversity in pulse duration and focusing.

In which there is consensus is the fluence/intensity dependence of the dimensions of the ablated holes [18,34,37,39]. The diameter/depth vs. intensity functions in Figs. 3(a)–3(f) show the well documented behavior: a rapid increase in depth and diameter above threshold followed by leveling for depth and linear increase with a moderate slope for diameter [e.g. 34]. The evolution of the transient reflectivity in Figs. 3(g)–3(i) further substantiates the conclusion of the authors [34] that the change in the ablation characteristics is due to plasma formation. The increase in reflectivity explains the saturation of the growth in the ablated volume normalized to pulse energy described by Varkentina et al. [17] as well.

Another firmly confirmed trend refers to the dependence of the ablation threshold on pulse duration: Studies performed in the 7–300 fs domain [33,37] suggest that when keeping the spot area fixed increasing pulse duration leads to an increase in the threshold fluence. In terms of intensity this relation behaves the opposite way: the thresholds decrease with increasing pulse duration [33,37]. Comparison of the absolute values of the thresholds is still a challenge because of the differences in process parameters. Chimier et al. [33] Hoffart et al. [37] and Xu et al. [39] report very similar thresholds: around 2.5 J/cm^2 & 0.8 × 10^{14} W/cm^2 (cf. Table 1). These values are roughly half of those derived for the three glasses.

Table 1. Compilation of ablation threshold data related to fused silica and glasses reported in the literature.

Reference	[35]	[33]	[34]	[37]	[39]	[16]	[30]	[42]	[17]	[44]	[38]	[48]	[42]	[49]	[41]	[51]
Material	fused silica									Borofloat		Soda-lime	BK7		Corning 0211	ASG, SLG and BSG^b
Pulse duration (fs)	5	7, 30, 100 and 300	7 - 300	7, 30 and 100	35	120	100-2000	150	450	120	200	150	150		600	800
Spot radius (μm)	70.7		4.65		43	25/38^a	4	2	4.65	10.7	16.2	5.92	2	17	-	1.5
Wavelength (nm)	780			800				775	1025	800	780	775	800		527 and 1053	1552
Thresholds (J/cm^2)	4.9	1.2, 2.4, 3.4 and 4.2	1.3-4.5	1.25, 2.43 and 3.7	2.6	5.4	4.0-6.0	4.4	5.9	2.8-4.25	4.4	2.55	2.42	5.6	59 and 1271 nJ	2.53, 5.34 and 7.23

^{a}minor/major, ^{b}aluminosilicate glass, soda-lime glass and borosilicate glass

What is unexplored yet is the effect of the spot dimensions on the ablation characteristics. Thresholds range from 2.6 J/cm^2 (0.74 × 10^{14} Wcm^{-2}) [39] to 5.4 J/cm^2 (0.45 × 10^{14} W/cm^2) [33,

37 and 16]. Systematic studies intended for the clarification of the effect of spot dimensions on the ablation characteristics would be most welcome.

Results on glasses ablated by fs pulses are scarce [38,41,42,48–51] (cf. Table 1). The thresholds reported scatter between 2.53 - 7.23 J/cm^2 depending on the process parameters. Taking into account that Ben-Yakar et al. [48] defined Φ_{th} as $E_p/\pi w^2$ and worked at 200 fs, the 2.55 J/cm^2 threshold corresponding to 2.55×10^{13} W/cm^2 fits fairy well our 5.85 J/cm^2 ($1.72 \pm 0.06 \times 10^{14}$ W/cm^2) value. Grehn et al. [38] report 4.4 J/cm^2 (3.66×10^{13} W/cm^2) as the $2E_p/\pi w^2$ ablation threshold of the Borofloat glass. The intensities are below ours due to the higher pulse durations. The 5.6 J/cm^2 (3.7×10^{13} W/cm^2) thresholds given by Campbell et al. for BK7 [49] and the 4.9-5.7 J/cm^2 range of thresholds reported by Lee et al. [51] for soda-lime glass matches our 5.85-6.42 J/cm^2 domain.

In summary: According to our results the thresholds derived for Borofloat, BK7 and soda-lime glasses are the same within experimental error. Whenever comparison is feasible, the glass thresholds prove to be systematically higher than those of fused silica: For pulse durations around 30 fs, the fluence threshold of the glasses is approximately two times higher. In the 100-300 fs domain the tendency remains: the 4.4-5.6 J/cm^2 values reported for glasses [38,48,49] exceed the 3.4-4.5 J/cm^2 fused silica thresholds [33,34,37].

4.2. Transient optical response

As the ratios of the measured (PD) to extrapolated permanent (PD$_{permanent}$) signal values (dotted vs. continuous lines in Figs. 3(g)–3(i) and Fig. 4(a) give the ratios of the transient to permanent reflectivity, the enhancement in reflectivity is defined as (PD-PD$_{permanent}$)/ PD$_{permanent}$. Below plasma threshold the data points should be zero by definition. The negative values come from the measurement error in photodiode signal, PD. According to Fig. 4(b) the reflectivity above threshold increases with >400, ~200 and ~130% at 8×10^{14} W/cm^2 as compared to the respective permanent reflectivities for Borofloat, BK7 and B270, respectively. The rate of enhancement in reflectivity at intensities exceeding the threshold is the highest in the case of the Borofloat, the BK7 and B270 possessing less increase as quantified by the slopes (a_t) of the straight lines fitted to the measured data: dotted lines in Fig. 4(a). The transient reflectivity of the B270 glass reaches its maximum with ~150% at around 6×10^{14} W/cm^2, decreasing with further increase in the intensity. Leveling characterizes the behavior of BK7 while the increase in the reflectivity measured in the case of the Borofloat glass does not reach its maximum in the intensity domain investigated.

The time integrated transient reflectivity results reported in literature are dominated by studies on fused silica as well. Both Ziener et al. [10] and Dromey et al. [15] report an increase from 0.04 at 6×10^{13} W/cm^2 up to 0.8 at 3×10^{15} W/cm^2 followed by leveling and dropping down above 10^{16} W/cm^2 for 90 fs@800 nm pulses under an incident angle of 6°. For the angle of incidence of 18° the reflectivity rises from 0.04 to 0.75, while for 45° it reaches 0.65 starting from ~0.02 [10]. For 60 fs@800 nm pulses, s-polarisation, at 45° Doumy et al. [11] report reflectivity values increasing from 0.1 to 0.7 as a function of fluence. With similar incidence conditions 7 fs@730 nm pulses induce an increase from ~0.07 to 0.6 for s-polarized and an increase from ~0.005 to 0.37 for p-polarized beam [12].

The transient reflectivity enhancements of 400, 200 and 150% (Fig. 4(b)) are associated with maximum reflectivity values of 0.034, 0.027 and 0.023 at intensities of 8×10^{14}, 6×10^{14} and 6×10^{14} W/cm^2 for Borofloat, BK7 and B270, respectively. These values are much less than those reported for fused silica [10–12,15], which is realistic taking into account that our measurements were performed at 45° incidence, p-polarization and in a lower intensity domain. Nevertheless, since the spot radii of the processing beam (7.5 μm [12], 15 μm [11] and >100 μm [10,15]) differ considerably from our 25 ± 2 μm value the comparison of the absolute values of the reflectivity is not really straightforward.
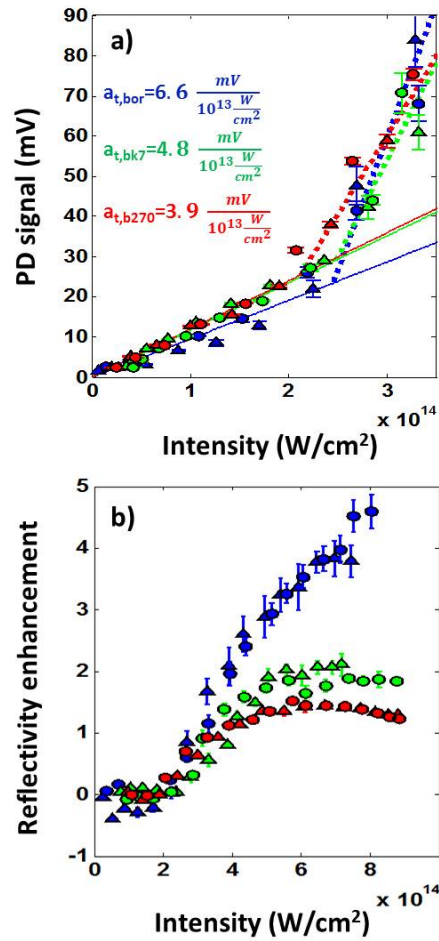
Fig. 4. The low intensity parts of the PD signal vs. intensity curves (a) and the enhancement in reflectivity defined as (PD-PD$_{permanent}$)/PD$_{permanent}$ (b) for Borofloat (blue), BK7 (green) and B270 (red) glasses.

The comparison of the enhancement in reflectivity [17] is however a viable approach. The increase in reflectivity recorded for BK7 (Fig. 4(b)) matches perfectly the value reported in [17] describing an increase from 0.068 to 0.2 in the transient reflectivity meaning an enhancement of 200% when ablating fused silica by 500 fs@1025 nm pulses. In the case of fused silica the steep increase in reflectivity starts when the fluence exceeds ~1.5 times the ablation threshold, Φ_{th} while the reflectivity maximum is reached at $5\Phi_{th}$ with saturation after. Despite the differences in both the material and pulse duration the BK7 possesses exactly the same characteristics: at low fluencies until ~1.5Φ_{th} the constant reflectivity values indicate the lack of dense plasma formation. Above this fluence the reflectivity increases rapidly until 200%, marking dense plasma formation acting as plasma mirror. The explanation of the saturation of the reflectivity above ~4.5Φ_{th} remains open.

The different growing rates of the reflectivity enhancement vs. intensity curves above the ablation threshold in Fig. 4(b) indicate that the characteristics of the plasma mirrors formed are different in the case of the three glasses investigated.

4.3. The origin of the reflectivity behavior

In a quest for understanding the origin of the differences the relation between the reflectivity and the amount of material ablated was first assessed. In calculating the volume of the ablated material the shape of the ablated region was assumed to be an elliptic cylinder the volume of which was calculated as $V=(d^2 \pi \sqrt{2}/4)h$, where d and h denote the smaller diameter and the depth of the ablated spot, respectively. While this approximation results in a small overestimation at low intensities where the shape is Gaussian-like, but is sufficiently correct at high intensities where the shape can be well approached by a cylinder, it is appropriate for comparison.

As seen in Fig. 5 the ablated volume increases linearly with increasing pulse energy up to ~250 µJ for all three glasses. Since this value marks the onset of the saturation in ablated hole depth (c.f. Figs. 3(d)–3(f)) above this energy the rise in ablated volume slows down. At the highest pulse energies roughly 550 µm^3 material is ablated in all cases. The similarity of the three curves supports again that the three glasses behave akin from the point of view of ablation and suggests thereby that the differences in the intensity dependence of the reflectivity cannot be correlated with the dependence of the ablated volume.
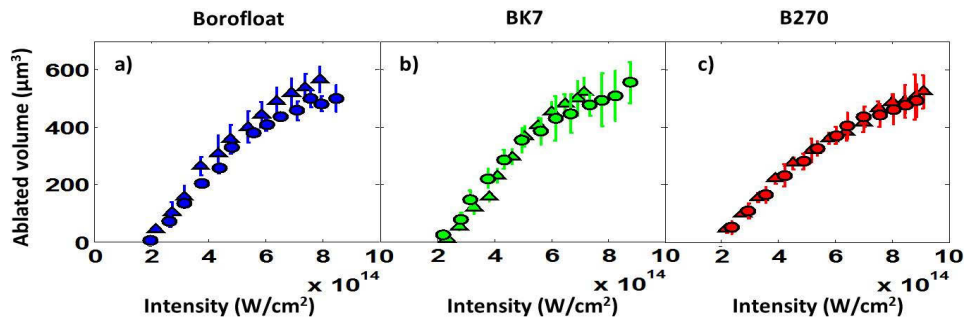

Fig. 5. The ablated volume as a function of the pulse energy for a) BOROFLOAT b) BK7 and c) B270.

The differences in the measured PD signal vs. ablated volume functions (Fig. 6) support more directly this statement. Up to ~250 µm^3 the PD signal increases approximately linearly with the ablated volume for all three glasses. Above this threshold linearity is kept for B270, a steeper increase sets on for BK7, Borofloat producing the highest increase in reflectivity. The behavior of the reflectivity as a function of ablated volume further substantiates that the volume is not the parameter that could explain the observed differences.
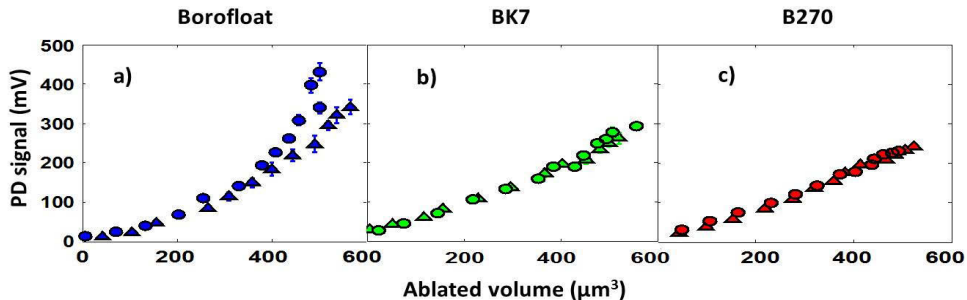

Fig. 6. The reflected signal as a function of the ablated volume for a) BOROFLOAT b) BK7 c) B270.

To understand the observed discrepancies, it should be kept in mind that the time scale and therefore the processes involved in plasma mirror formation and material removal are significantly different [57]. By measuring the reflectivity of the ablating femtosecond pulse we examine the first step which explains why the volume approach failed.

Grehn et al. [38] explained the composition dependence of the ablation characteristics by the difference in the average dissociation energies of the glasses. In our case these energies proved to be similar, in line with the similarity of the ablation thresholds measured. Extending this approach for the explanation of the optical characteristics, we estimated the average number of electrons, $n_{e,av}$, participating in the formation of 1 mol glass for describing the composition dependence of the reflectivity. The numbers of electrons calculated according to the molar concentration of all subunits together with the composition of the respective glasses are summarized in Table 2.

Table 2. Composition and the calculated average electron number ($n_{e, av}$) of the investigated glasses and fused silica.

Material	Constituents (wt%)											$n_{e,av}$
	SiO_2	B_2O_3	Na_2O	K_2O	CaO	ZnO	BaO	Al_2O_3	As_2O_3	TiO_2	Sb_2O_3	
BOROFLOAT[a]	81	13	4		-	-	-	2	-	-	-	4.19
BK7[b]	70	10	10	6	-	-	3	-	1	-	-	3.91
B270[c]	69	-	8	8	7	4	2	-	-	1	1	3.48
Fused silica	100	-	-	-	-	-	-	-	-	-	-	4.0

[a]data provided by Schott
[b]data provided by Eksma Optics and [58]
[c]data from [59]

According to the calculation most electrons are involved in the formation of the Borofloat glass which actually exhibits the highest plasma mirror reflectivity. With 3.91 BK7 possesses the second highest, while B270 with 3.48 shows the lowest reflectivity. It can be concluded thereby that the variation in the integrated plasma mirror reflectivity well correlates with the average number of electrons involved in the glass formation. With 4.0 the average electron number of fused silica is nearest to that of BK7, 3.91. The reflectivity enhancement reported for fused silica [17] is identical to the measured enhancements in Fig. 4(b) for BK7, further supporting that the similarity in the numbers of bond electrons involved in the plasma formation induces akin reflectivity enhancements proving that our electron number approach offers a plausible explanation for the differences observed in the reflectivity values of the three glasses investigated.

5. Conclusion

The Borofloat, BK7 and B270 glasses behave similarly from the point of view of ablation. The intensity thresholds lie in the $1.7\text{-}1.9 \times 10^{14}$ W/cm^2 domain. Above threshold the diameter values follow logarithmic dependence. The depths saturate above 5×10^{14} W/cm^2 with 250, 240 and 220 nm for Borofloat, BK7 and B270, respectively. Comparison of the few glass ablation threshold values available in the literature is not straightforward due to the high scatter in pulse durations and spot sizes, nevertheless our results suggest that the glasses investigated exhibit higher ablation thresholds as compared to that of fused silica.

The high intensity optical response of the glasses is different. The Borofloat glass possesses the steepest increase in time integrated transient reflectivity with intensity. The difference in the average number of electrons participating in the formation of 1 mole glass gives a plausible explanation for the differences in the reflectivity.

The message of the comparison of the ablation and optical characteristics in the high intensity domain is that the knowledge of the answer of the material to ablation is not enough to predict the

optical response. Optical glasses can be good plasma mirror hosts because of uniformly shallow holes and with reflectivity enhancement comparing favorably with that of fused silica. Out of the three glasses the highest transient reflectivity prefers Borofloat as potential plasma mirror target.

Disclosures

The authors declare no conflicts of interest.

References

1. H. C. Kapteyn, M. M. Murname, A. Szoke, and R. W. Falcone, "Prepulse energy suppression for high-energy ultrashort pulses using self-induced plasma shuttering," Opt. Lett. **16**(7), 490–492 (1991).
2. S. Backus, H. C. Kapteyn, M. M. Murname, D. M. Gold, H. Nathel, and W. White, "Prepulse suppression for high-energy ultrashort pulses using self-induced plasma shuttering from fluid target," Opt. Lett. **18**(2), 134–136 (1993).
3. D. M. Gold, "Direct measurement of prepulse suppression by use of a plasma shutter," Opt. Lett. **19**(23), 2006–2008 (1994).
4. Z. Bor, B. Racz, G. Szabo, D. Xenakis, C. Kalpouzos, and C. Fotakis, "Femtosecond transient reflection from polymer surfaces during femtosecond UV photoablation," Appl. Phys. A **60**(4), 365–368 (1995).
5. B. Hopp, Z. Tóth, K. Gál, Á. Mechler, Z. Bor, S. D. Moustaizis, S. Georgiou, and C. Fotakis, "Time-resolved investigation of the transient surfaces reflection changes of subpicosecond excimer laser ablated liquids," Appl. Phys. A **69**(7), S191–S194 (1999).
6. B. Gilicze, A. Barna, Z. Kovács, S. Szatmári, and I. B. Földes, "Plasma mirrors for short pulse KrF lasers," Rev. Sci. Instrum. **87**(8), 083101 (2016).
7. D. Du, X. Liu, G. Korn, J. Squier, and G. Mourou, "Laserinduced breakdown by impact ionization in SiO2 with pulse widths from 7 ns to 150 fs," Appl. Phys. Lett. **64**(23), 3071–3073 (1994).
8. D. von der Linde and H. Schüler, "Breakdown threshold and plasma formation in femtosecond laser-solid interaction," J. Opt. Soc. Am. B **13**(1), 216–222 (1996).
9. E. G. Gamaly, A. V. Rode, B. Luther-Davies, and V. T. Tikhonchuk, "Ablation of solids by femtosecond lasers: "Ablation mechanism and ablation thresholds for metals and dielectrics," Phys. Plasmas **9**(3), 949–957 (2002).
10. Ch. Ziener, P. S. Foster, E. J. Divall, C. J. Hooker, M. H. R. Hutchinson, A. J. Langley, and D. Neely, "Specular reflectivity of plasma mirrors as a function of intensity, pulse duration, and angle of incidence," J. Appl. Phys. **93**(1), 768–770 (2003).
11. G. Doumy, F. Quéré, O. Gobert, M. Pedrix, P. Martin, P. Audebert, J. C. Gauthier, J.-P. Geindre, and T. Wittmann, "Complete characterization of a plasma mirror for the production of high-contrast ultraintense laser pulses," Phys. Rev. E **69**(2), 026402 (2004).
12. Y. Nomura, L. Veisz, K. Schmid, T. Wittmann, J. Wild, and F. Krausz, "Time-resolved reflectivity measurements on a plasma mirror with few-cycle laser pulses," New J. Phys. **9**(1), 9 (2007).
13. T. Wittmann, J. P. Geindre, P. Audebert, R. S. Marjoribanks, J. P. Rousseau, F. Burgy, D. Douillet, T. Lefrou, K. TaPhuoc, and J. P. Chambaret, "Towards ultrahigh-contrast ultraintense laser pulses-complete characterization of a double plasma-mirror pulse cleaner," Rev. Sci. Instrum. **77**(8), 083109 (2006).
14. S. Inoue, K. Maeda, S. Tokita, K. Mori, K. Teramoto, M. Hashida, and S. Sakabe, "Single plasma mirror providing 10^4 contrast enhancement and 70% reflectivity for intense femtosecond lasers," Appl. Opt. **55**(21), 5647–5651 (2016).
15. B. Dromey, S. Kar, M. Zepf, and P. Foster, "The plasma mirror—A subpicosecond optical switch for ultrahigh power lasers," Rev. Sci. Instrum. **75**(3), 645–649 (2004).
16. D. Puerto, J. Siegel, W. Gawelda, M. Galvan-Sosa, I. Ehrentraut, J. Bonse, and J. Solis, "Dynamics of plasma formation, relaxation, and topography modification induced by femtosecond laser pulses in crystalline and amorphous dielectrics," J. Opt. Soc. Am. B **27**(5), 1065–1076 (2010).
17. N. Varkentina, N. Sanner, M. Lebugle, M. Sentis, and O. Utéza, "Absorption of a single 500 fs laser pulse at the surface of fused silica: Energy balance and ablation efficiency," J. Appl. Phys. **114**(17), 173105 (2013).
18. M. Lebugle, N. Sanner, N. Varkentina, M. Sentis, and O. Utéza, "Dynamics of femtosecond laser absorption of fused silica in the ablation regime," J. Appl. Phys. **116**(6), 063105 (2014).

19. L. Haahr-Lillevang, K. Waedegaard, D. B. Sandkamm, A. Mouskeftaras, S. Guizard, and P. Balling, "Short-pulse laser excitation of quartz: experiments and modeling of transient optical properties and ablation," Appl. Phys. A **120**(4), 1221–1227 (2015).

20. D. Panasenko, A. J. Shu, A. Gonsalves, K. Nakamura, N. H. Patlis, C. Toth, and W. P. Leemans, "Demonstration of a plasma mirror based on a laminar flow water film," J. Appl. Phys. **108**(4), 044913 (2010).

21. P. L. Poole, C. Wilis, G. E. Cochran, R. T. Hanna, C. D. Andereck, and D. W. Schumacher, "Moderate repetition rate ultra-intense laser targets and optics using variable thickness liquid crystal films," Appl. Phys. Lett. **109**(15), 151109 (2016).

22. B. H. Shaw, S. Steinke, J. van Tillborg, and W. P. Leemans, "Reflectance characterization of tape-based plasma mirrors," Phys. Plasmas **23**(6), 063118 (2016).

23. A. Borot, A. Malvache, X. Chen, D. Douillet, G. Iaquianiello, T. Lefrou, P. Audebert, J.-P. Geindre, G. Mourou, F. Quéré, and R. L. Martens, "High-harmonic generation from plasma mirrors at kilohertz repetition rate," Opt. Lett. **36**(8), 1461–1463 (2011).

24. G. G. Scott, V. Bagnoud, C. Brabetz, R. J. Clarke, J. S. Green, R. I. Heathcote, H. W. Powell, B. Zielbauer, T. D. Arber, P. McKenna, and D. Neely, "Optimization of plasma mirror reflectivity and optical quality using double laser pulses," New J. Phys. **17**(3), 033027 (2015).

25. B. C. Stuart, M. D. Feit, A. M. Rubenchik, B. W. Shore, and M. D. Perry, "Laser-induced damage in dielectrics with nanosecond to subpicosecond pulses," Phys. Rev. Lett. **74**(12), 2248–2251 (1995).

26. W. Kautek, J. Krüger, M. Lenzner, S. Sartania, C. Spielmann, and F. Krausz, "Laser ablation of dielectrics with pulse durations between 20 fs and 3 ps," Appl. Phys. Lett. **69**(21), 3146–3148 (1996).

27. D. Ashkenasi, A. Rosenfeld, H. Varel, M. Wahmer, and E. E. B. Campbell, "Laser processing of sapphire with picosecond and sub-picosecond pulses," Appl. Surf. Sci. **120**(1-2), 65–80 (1997).

28. J. Krüger, W. Kautek, M. Lenzner, S. Sartania, C. Spielmann, and F. Krausz, "Laser micromachining of barium aluminium borosilicate glass with pulse durations between 20 fs and 3 ps," Appl. Surf. Sci. **127-129**, 892–898 (1998).

29. M. Lenzner, J. Krüger, S. Sartania, Z. Cheng, C. Spielmann, G. Mourou, W. Kautek, and F. Krausz, "Femtosecond optical breakdown in dielectrics," Phys. Rev. Lett. **80**(18), 4076–4079 (1998).

30. D. Giguére, G. Olivié, F. Vidal, S. Toetsch, G. Girard, T. Ozaki, and J. C. Kieffer, "Laser ablation threshold dependence on pulse duration for fused silica and corneal tissues: experiments and modeling," J. Opt. Soc. Am. A **24**(6), 1562–1568 (2007).

31. O. Utéza, B. Bussiére, F. Canova, J.-P. Chambaret, P. Delaporte, T. Itina, and M. Sentis, "Laser-induced damaged threshold of sapphire in nanosecond, picosecond and femtosecond regimes," Appl. Surf. Sci. **254**(4), 799–803 (2007).

32. N. Sanner, O. Utéza, B. Chimier, M. Sentis, P. Lassondé, F. Légaré, and J. C. Kieffer, "Toward determinism in surface damaging of dielectrics using few-cycle laser pulses," Appl. Phys. Lett. **96**(7), 071111 (2010).

33. B. Chimier, O. Utéza, N. Sanner, M. Sentis, T. Itina, P. Lassonde, F. Légaré, F. Vidal, and J. C. Kieffer, "Damage and ablation thresholds of fused silica in femtosecond regime," Phys. Rev. B **84**(9), 094104 (2011).

34. O. Utéza, N. Sanner, B. Chimier, A. Brocas, N. Varkentina, M. Sentis, P. Lassonde, F. Légaré, and J. C. Kieffer, "Control of material removal of fused silica with single pulses of few optical cycles to sub-picosecond duration," Appl. Phys. A **105**(1), 131–141 (2011).

35. M. Lenzner, J. Krüger, W. Kautek, and F. Krausz, "Precision laser ablation of dielectrics in the 10-fs regime," Appl. Phys. A **68**(3), 369–371 (1999).

36. B. N. Chickhov, C. Momma, S. Nolte, F. von Alvensleben, and A. Tünnermann, "Femtosecond, picosecond and nanosecond laser ablation of solids," Appl. Phys. A **63**(2), 109–115 (1996).

37. L. Hoffart, P. Lassonde, F. Légaré, F. Vidal, N. Sanner, O. Utéza, M. Sentis, J.-C. Kieffer, and I. Brunette, "Surface ablation of corneal stroma with few-cycle laser pulses at 800 nm," Opt. Express **19**(1), 230–240 (2011).

38. M. Grehn, T. Seuthe, M. Höfner, N. Griga, C. Theiss, A. Mermillod-Blondin, M. Eberstein, H. Eichler, and J. Bonse, "Femtosecond-laser induced ablation of silicate glasses and the intrinsic dissociation energy," Opt. Mater. Express **4**(4), 689–700 (2014).

39. S.-Z. Xu, C.-Z. Yao, W. Liao, X.-D. Yuan, T. Wang, and X.-T. Zu, "Experimental study on 800 nm femtoscond laser ablation of fused silica in air and vacuum," Nucl. Instrum. Methods Phys. Res., Sect. B **385**, 46–50 (2016).

40. A. Rosenfeld, D. Ashkenasi, H. Varel, M. Wahmer, and E. E. B. Campbell, "Time resolved detection of particle removal from dielectrics on femtosecond laser ablation," Appl. Surf. Sci. **127-129**, 76–80 (1998).

41. A. P. Joglekar, H. Liu, G. J. Spooner, E. Meyhöfer, G. Mourou, and A. J. Hunt, "A study of the deterministic character of optical damage by femtosecond laser pulses and applications to nanomachining," Appl. Phys. B **77**(1), 25–30 (2003).

42. D. F. Farson, H. W. Choi, B. Zimmerman, J. K. Steach, J. J. Chalmers, S. V. Olesik, and L. J. Lee, "Femtosecond laser micromachining of dielectric materials for biomedical applications," J. Micromech. Microeng. **18**(3), 035020 (2008).

43. N. Sanner, B. Bussiere, O. Utéza, A. Leray, T. Itina, M. Sentis, J. Y. Natoli, and M. Commandré, "Influence of the beam-focus size on femtosecond laser-induced damage threshold in fused silica," Proc. SPIE **6881**, 68810W (2008).

44. N. Sanner, O. Utéza, B. Bussiere, G. Coustillier, A. Leray, T. Itina, and M. Sentis, "Measurement of femtosecond laser-induced damage and ablation thresholds in dielectrics," Appl. Phys. A **94**(4), 889–897 (2009).

45. M. H. Shaheen, J. E. Gagnon, and B. J. Fryer, "Femtosecond laser ablation behavior of gold, crystalline silicon, and fused silica: a comparative study," Laser Phys. **24**(10), 106102 (2014).

46. M. S. Rafique, S. Bashir, W. Husinsky, A. Hobro, and B. Lendl, "Surface analysis correlated with the Raman measurements of a femtosecond laser irradiated CaF$_2$," Appl. Surf. Sci. **258**(7), 3178–3183 (2012).

47. S. Guizard, A. Semerok, J. Gaudin, M. Hashida, P. Martin, and F. Quéré, "Femtosecond laser ablation of transparent dielectrics: measurement and modelisation of crater profiles," Appl. Surf. Sci. **186**(1-4), 364–368 (2002).

48. A. Ben-Yakar and R. L. Byer, "Femtosecond laser ablation properties of borosilicate glass," J. Appl. Phys. **96**(9), 5316–5323 (2004).

49. S. Campbell, F. C. Dear, D. P. Hand, and D. T. Reid, "Single-pulse femtosecond laser machining of glass," J. Opt. A: Pure Appl. Opt. **7**(4), 162–168 (2005).

50. P. K. Diwakar, J. J. Gonzalez, S. S. Harilal, R. E. Russo, and A. Hassanein, "Ultrafast laser ablation ICP-MS: Role of spot size, laser fluence, and repetition rate on signal intensity and elemental fractionation," J. Anal. At. Spectrom. **29**(2), 339–346 (2014).

51. H.-M. Lee, J. H. Choi, and S.-J. Moon, "Effect of the chemical composition on the ablation characteristics of glass substrates in femtosecond laser machining," Int. J. Precis. Eng. Manuf. **18**(11), 1495–1499 (2017).

52. C. Mullan, G. M. O'Connor, S. Favre, D. Ilie, and T. J. Glynn, "Estimating spot size and relating hole diameters with fluence and number of shots for nanosecond and femtosecond laser ablation polyethylene terephthalate," J. Laser Appl. **19**(3), 158–164 (2007).

53. C. D. Marco, S. M. Eaton, R. Suriano, S. Turri, M. Levi, R. Ramponi, G. Cerullo, and R. Osellame, "Surface properties of femtosecond laser ablated PMMA," ACS Appl. Mater. Interfaces **2**(8), 2377–2384 (2010).

54. Official webpage of TeWaTi lab, http://tewati.physx.u-szeged.hu/index.php/en/ Date of access: 09. 23. 2019.

55. J. M. Liu, "Simple technique for measurements of pulsed Gaussian-beam spot sizes," Opt. Lett. **7**(5), 196–198 (1982).

56. J. Krüger, M. Lenzner, S. Martin, M. Lenner, C. Spielmann, A. Fiedler, and W. Kautek, "Single- and multi-pulse femtosecond laser ablation of optical filter materials," Appl. Surf. Sci. **208-209**, 233–237 (2003).

57. B. Rethfeld, K. Sokolowski-Tinten, D. von der Linde, and S. I. Anisimov, "Timescales in the response of materials to femtosecond laser excitation," Appl. Phys. A **79**(4-6), 767–769 (2004).

58. H. Zhenguang, R. Srivastava, and R. V. Ramaswamy, "Low-loss small-mode passive waveguides and near-adiabatic tapers in BK7 glass," J. Lightwave Technol. **7**(10), 1590–1596 (1989).

59. J. Kent and M. Tsumura, "Acoustic touch position sensor using a low acoustic loss transparent substrate," (US Patent US6236391B1). https://patents.google.com/patent/US6236391B1/en